Vortex revivals and Fermi-Pasta-Ulam-Tsingou recurrence

Angel Paredes,[1] José Blanco-Labrador,[1] David N. Olivieri,[2] José R. Salgueiro,[1] and Humberto Michinel[1]
[1]*Departamento de Física Aplicada, Universidade de Vigo, As Lagoas s/n, Ourense, ES-32004 Spain*
[2]*Departamento de Linguaxes e Sistemas Informáticos, Universidade de Vigo, As Lagoas s/n, Ourense, ES-32004 Spain*

(Received 18 December 2018; revised manuscript received 4 March 2019; published 14 June 2019)

We study the self-trapped vortex-ring eigenstates of the two-dimensional Schrödinger equation with focusing Poisson and cubic nonlinearities. For each value of the topological charge l, there is a family of solutions depending on a parameter that can be understood as the relative importance of the cubic term. We analyze the perturbative stability of the solutions and simulate the fate of the unstable ones. For $l = 1$ and $l = 2$, there is an interval of the family of eigenstates for which the initial profile breaks apart but subsequently reconstructs itself, a process that can be interpreted as a nontrivial nonlinear oscillation between the vortex and an azimuthon. This revival provides a compelling realization of a recurrence of the Fermi-Pasta-Ulam-Tsingou type. Outside this interval, the vortices can be stable (for small cubic terms) or unstable and nonrecurrent (for large cubic terms). We argue that there is a crossover between these regimes that resembles a strong stochasticity threshold. For $l \geqslant 3$, all solutions are unstable and nonrecurrent. Finally, we comment on the possible experimental implementation of this phenomenon in the context of nonlinear laser beam propagation in thermo-optical media.

DOI: 10.1103/PhysRevE.99.062211

I. INTRODUCTION

The discoveries put forward in the seminal contribution [1] initiated the field of "numerical experimentation" and were decisive in the development of the theories of integrability, solitons, and chaos [2–4]. By simulating a one-dimensional (1D) array of coupled nonlinear oscillators, the authors intended to observe the onset of thermalization by exciting a given mode and computing how evolution would result in energy equipartition. To their surprise, they found that, even if energy was initially transferred to other modes, the initial state was almost perfectly reconstructed after some time. This seemingly paradoxical behavior is called the Fermi-Pasta-Ulam-Tsingou (FPUT) [5] recurrence and, remarkably, a similar phenomenon has been found to occur in particular circumstances for the nonlinear evolution of widely disparate physical systems, e.g., oceanic waves [6] and gravitating matter fields [7].

Integrability plays a major role in the interpretation of the FPUT dynamics and, in this context, the one-dimensional nonlinear Schrödinger equation (NLSE) has been a particularly relevant model. Various analytic solutions [8,9] explicitly show how modulation instability distorts a wave envelope that after nonlinear evolution eventually recovers its original form. These classical results were later interpreted from the FPUT viewpoint [10,11]. Recurrences stemming from the 1D NLSE have been observed experimentally in hydrodynamics [12,13] and in the spatial [14] and temporal [12,15,16] dynamics of laser pulses, even in the presence of third-order dispersion [17] and dissipation [13]. It is known that nonlinear recurrences also appear for nonintegrable systems, typically in relation to weak chaos [18]. Connection between FPUT-like dynamics and nonintegrable versions of the NLSE have been studied in Refs. [19,20].

In two- and three-dimensional setups, NLSE nontrivial revivals of an initial profile have been found in a number of remarkable papers. In fact, oscillations between vortex rings and azimuthons that share qualitative similarities with the present discussion were put forward in Ref. [21]. In Refs. [22,23], periodic transformations between higher-order solitons with nonlocal nonlinearities were found numerically. Revivals of dark solitary waves have also been described: In Ref. [24], the decay and reconstruction of ring dark solitons was found in a particular situation. Interestingly, the change of the stability properties of those states on the tuning of the potential was analyzed in Ref. [25]. Moreover, the oscillation between a dark soliton and a ring of vortices in a three-dimensional setup was implemented experimentally in Ref. [26].

The goal of this contribution is to present an interesting case of nonlinear recurrences in a far from integrable version of the NLSE and to put forward its qualitative similarities to FPUT. We do so by numerically studying the self-trapped vortex-ring eigenstates of the two-dimensional NLSE with focusing Poisson and cubic nonlinearities. Vortex-ring solitons are nonlinear solutions with screw topological phase dislocations [27,28] that have attracted much attention, especially in nonlinear optics [29,30]. (Notice that the term "vortex ring" has been used in the literature for different types of configurations. In the present case, it refers to a two-dimensional radially symmetric energy distribution of finite extent that surrounds a phase singularity.) We find that recurrences happen for a class of such states with topological charges $l = 1, 2$: The vortex is linearly unstable under azimuthal perturbations that modulate the initial profile and lead to a configuration that can be interpreted as a system of two or three equal solitons that orbit around each other, namely an azimuthon [31,32]. On nonlinear evolution, the unstable radially symmetric eigenstate gets nontrivially reconstructed.

 ©2019 American Physical Society

In particular, many cycles of destruction and revival occur for $l = 1$.

In the following, we study the aforementioned families of eigenstates that, besides the ordinary behaviors of stability and nonrecurrent instability [33], include these interesting perturbatively unstable but robust FPUT-recurrent vortex rings. In Sec. II, we introduce the vortex-ring eigenstates and discuss their perturbative stability. Section III presents results of numerical integration that allow us to discuss the fate of the unstable initial conditions, including cases with repeated revivals. In Sec. IV we look for connections with peculiar features of FPUT systems. Section V briefly discusses a plausible realization of the mathematical model for a particular nonlinear optical setup. Finally, in Sec. VI we summarize the discussion and outline some open questions for future investigation.

II. MATHEMATICAL MODEL, SELF-TRAPPED VORTEX EIGENSTATES AND PERTURBATIVE STABILITY

The two-dimensional NLSE with a focusing cubic and a Poisson term is given by:

$$i\frac{\partial\psi}{\partial z} = -\frac{1}{2}\nabla^2\psi - |\psi|^2\psi + \Phi\psi, \quad \nabla^2\Phi = 2\pi|\psi|^2. \tag{1}$$

Here the dimensional parameters have been absorbed, without loss of generality, by appropriately rescaling the wave function ψ, Poisson potential Φ, coordinates x, y, and propagation distance z [34]. Equation (1) must be supplemented with boundary conditions for Φ. In this paper, we consider conditions that preserve radial symmetry, $\Phi(r = r_{\rm ref}) = \Phi_0$, where $r_{\rm ref}$ is much larger than the size of the vortex ring (r and θ are the polar coordinates in the plane). The values of $r_{\rm ref}$ and Φ_0 are immaterial [34], since a constant shift $\Phi \to \Phi + c$ can be compensated by $\psi \to e^{-icz}\psi$. Propagation-invariant eigenstates take the form $\psi_{\rm vort} = e^{i\beta z}e^{il\theta}f(r)$, $\Phi_{\rm vort} = \phi(r)$, where l is an integer. The radial part of the two-dimensional Laplacian is defined as $\nabla_r^2 = \partial_r^2 + r^{-1}\partial_r$; absorbing the propagation constant in the Poisson potential $\varphi(r) = \phi(r) + \beta$, yields:

$$\varphi f = \frac{1}{2}\nabla_r^2 f - \frac{l^2}{2r^2}f + f^3, \qquad 2\pi f^2 = \nabla_r^2\varphi. \tag{2}$$

For $l \neq 0$, requiring regularity around $r = 0$ leads to $f(r) = f_0 r^{|l|} + \mathcal{O}(r^{|l|+2})$ and $\varphi(r) = \varphi_0 + \mathcal{O}(r^{2|l|+2})$, where f_0, φ_0 are integration constants. The physical eigenstates are the normalizable solutions [$\lim_{r\to\infty} f(r) = 0$]. Here we concentrate on the lowest-lying states, namely $f(r) > 0$ $\forall r > 0$ and use a standard shooting method to determine $\varphi_0(f_0)$. For each l, there exists a continuous family of solutions parameterized by $f_0 > 0$. In the $l = 0$ case [34], they vary between the Poisson-dominated limit [33] for $f_0 \to 0$ and the Poisson-less limit for $f_0 \to \infty$. Thus, f_0 can be physically interpreted as a parameter that dictates the relevance of the cubic term. The power and mean radius are given by:

$$P = 2\pi\int rf^2dr, \quad R = \frac{2\pi}{P}\int r^2f^2dr. \tag{3}$$

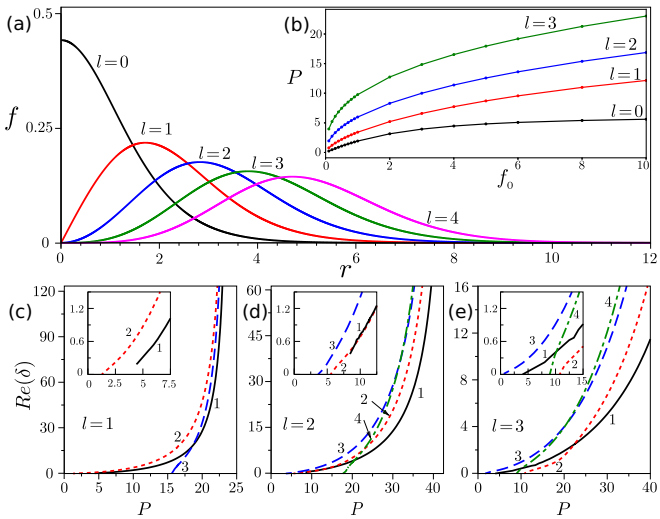

FIG. 1. Vortex-ring eigenstates. (a) Some eigenstates for $l = 0, \ldots, 4$. (b) The power P in terms of the parameter f_0. [(c)–(e)] Re(δ) as a function of P for $l = 1$, 2, 3, respectively. The integer associated with each line is the order of the azimuthal perturbation p. The solid line corresponds to $p = 1$, the dotted line to $p = 2$, the dashed line to $p = 3$, and the dot-dashed line to $p = 4$. The insets show more detailed views of the transition regions from stability [no solution with Re(δ) > 0] to perturbative instability. For $l \geqslant 3$, all solutions are unstable.

The angular momentum of an eigenstate is $J = Pl$. Some sample solutions and the numerically determined $P(f_0)$ are plotted in Fig. 1(a) and 1(b).

In order to study the linear stability of the eigenstates, we consider azimuthal perturbations of order p that take the following form [27,33]:

$$\begin{aligned}\psi(z, r, \theta) &= e^{i(\beta z + l\theta)}[f(r) + a(z, r)e^{ip\theta} + h(z, r)e^{-ip\theta}]\\ \Phi(z, r, \theta) &= \phi(r) + g(z, r)e^{ip\theta} + g^*(z, r)e^{-ip\theta},\end{aligned} \tag{4}$$

where $a(z, r)$, $h(z, r)$, and $g(z, r)$ are small complex amplitudes. Inserting these expressions into Eq. (1), we find the following linearized system for the perturbations:

$$\begin{aligned}i\partial_z a &= -\frac{\nabla_r^2 a}{2} + \left[\frac{(l+p)^2}{2r^2} - 2f^2 + \varphi\right]a - f^2h^* + fg,\\ i\partial_z h &= -\frac{\nabla_r^2 h}{2} + \left[\frac{(l-p)^2}{2r^2} - 2f^2 + \varphi\right]h - f^2a^* + fg^*,\\ \nabla_r^2 g &= \frac{p^2}{r^2}g + 2\pi f(a + h^*).\end{aligned} \tag{5}$$

This system can be solved by separating variables: $a(z, r) = [a_1(r) + ia_2(r)]e^{\delta z}$, $h(z, r) = [h_1(r) + ih_2(r)]e^{\delta^* z}$, $g(z, r) = [g_1(r) + ig_2(r)]e^{\delta z}$. This set of equations leads to an eigenvalue problem in δ amenable to a linear stability analysis [35]. We adopted a simpler and faster alternative method, commonly used in the past [36], based on the Crank-Nicolson scheme that evolves Eqs. (5) until the shapes of the functions $a(z, r)$, $h(z, r)$ do not change significantly. At every step in the algorithm, the function $g(r)$ is computed by finite differences and the system is rescaled by $|a|$ to avoid unbounded growth of the functions. For unstable eigenstates, the method

converges [Re(δ) > 0], where the eigenvalue is given by:

$$\mathrm{Re}(\delta) = \frac{1}{2\,\Delta z} \log \frac{|a(r, z+\Delta z)|^2}{|a(r,z)|^2}. \tag{6}$$

By repeatedly solving this system for the family of eigenstates, we compute Re(δ) for several values of l and p, see Figs. 1(c)–1(e). In the limit $f_0 \to 0$, the only stable vortices are those with $l = 1$ and 2 [33].

III. NONLINEAR EVOLUTION OF THE UNSTABLE SOLUTIONS AND VORTEX REVIVALS

In order to discuss the fate of the unstable solutions, we have repeatedly integrated Eqs. (1) using the vortex-ring eigenstates to define the initial conditions at $z = 0$. We used a standard split-step method, adapting the open-source code described in Ref. [37] to this particular case. The Poisson term of Eq. (1) is solved numerically at each step with a finite-difference method. For the perturbatively unstable vortices [see Figs. 1(c)–1(e)], the azimuthal perturbation grows and distorts the initial profile. Subsequently, however, different qualitative behaviors are observed. To conveniently compare and quantify the dynamics of different cases, we define the following parameter:

$$\sigma(z) = \frac{1}{P} \int |(|\psi_{\mathrm{vort}}|^2 - |\psi|^2)| d^2\mathbf{x}. \tag{7}$$

Thus $\sigma(z)$ characterizes the deviation of the power distribution at a given z from the initial eigenstate $|\psi_{\mathrm{vort}}|^2$. The definition of Eq. (7) implies $\sigma(z) \in [0, 2]$ since σ vanishes when $|\psi(z, x, y)| = |\psi_{\mathrm{vort}}(x, y)|$ and would be 2 if the support of the functions $|\psi(z, x, y)|$ and $|\psi_{\mathrm{vort}}(x, y)|$ were completely disjoint.

With topological charges $l = 1$, 2 and large values of f_0, the vortex-ring structure is rapidly destroyed after the azimuthal instability develops. The wave profile becomes disordered and part of the energy and angular momentum are radiated away. This familiar behavior is depicted in Fig. 2. All our simulations also indicated that the $l \geqslant 3$ solutions follow this same pattern.

For $l = 1$, 2 and for intermediate values of f_0, the splintered pieces from the initial vortex-ring orbit around each for a while, giving rise to an azimuthon [31,32]. Eventually, they merge again such that the unstable eigenstate is reconstructed with high precision, see Fig. 3. On further evolution, this cyclic process of vortex breaking and self-reconstruction is observed multiple times for a certain range of f_0. For such cases, total revivals robustly occur throughout very long simulation times.

Figure 4 shows an example of recurrence and eventual disintegration of an eigenstate with $l = 2$. Notice that, in this case, the ring splits in three pieces as predicted by the dominance of the $p = 3$ azimuthal perturbation, see Fig. 1(d).

The recurrences described here are numerically robust. We obtained qualitatively identical behavior by performing the simulations for different grid sizes as well as different z spacing (Δz) (i.e., tuning numerical precision in the computed evolution) or adding a limited amount of noise to the initial condition. At most, slight changes are appreciated in the onset times of perturbative instability growth, in the period between recurrences, and in the number of revivals before the appearance of the disordered phase.

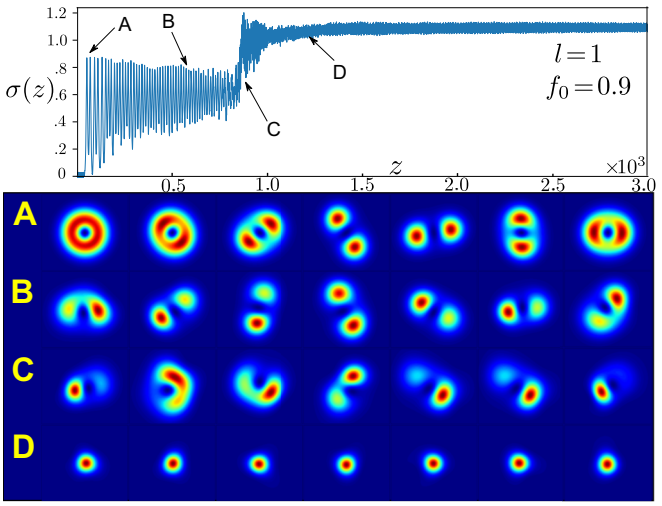

FIG. 2. An unstable nonrecurrent vortex. Top: An example ($l = 1$, $f_0 = 0.9$) of the long-distance evolution of $\sigma(z)$. Bottom: The two-dimensional profile of $|\psi_{\mathrm{vort}}|^2$ at different values of z. In region A there are partial revivals. Region B can be interpreted as the two pieces orbiting around each other (rotation is counter-clockwise), a behavior that becomes destabilized in region C. In (D), an $l = 0$ soliton remains, but surrounded by some radiation.

Figure 5 depicts a number of examples of $\sigma(z)$. We have found that recurrent solutions exist for $0.2 \lesssim f_0 \lesssim 0.6$ ($l = 1$) and $0.5 \lesssim f_0 \lesssim 0.8$ ($l = 2$). The lower bounds correspond to the onset of instability in the azimuthal perturbation, Fig. 1. As Fig. 5 shows, there is a crossover from the distinctly recurrent solutions to the distinctly nonrecurrent ones. Thus, the upper bounds of the intervals with recurrences are not sharply defined. In Sec. IV, we will identify this crossover with a strong stochasticity threshold. The recurrent behavior is clearly more robust for $l = 1$ than for $l = 2$. In the latter case, it comes to an end after a moderate number of cycles.

In the supplementary material [38], we provide representative videos displaying the described processes, including the cases of Figs. 2, 3, and 4.

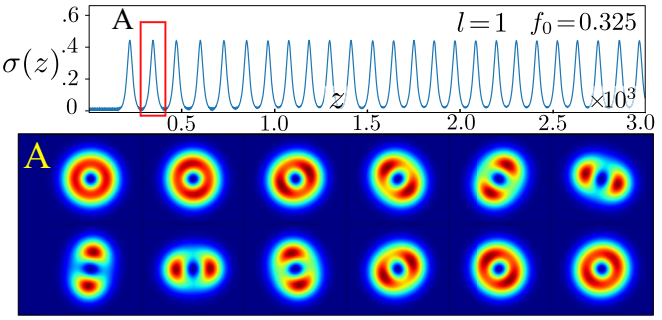

FIG. 3. A recurrent vortex. Top: An example ($l = 1$, $f_0 = 0.325$) of long-distance evolution of $\sigma(z)$. Bottom: The two-dimensional profile of $|\psi_{\mathrm{vort}}|^2$ for several values of z within the region A, indicated in the $\sigma(z)$ plot. The profiles show how the instability begins and breaks the beam into two pieces and how the initial state self-assembles.

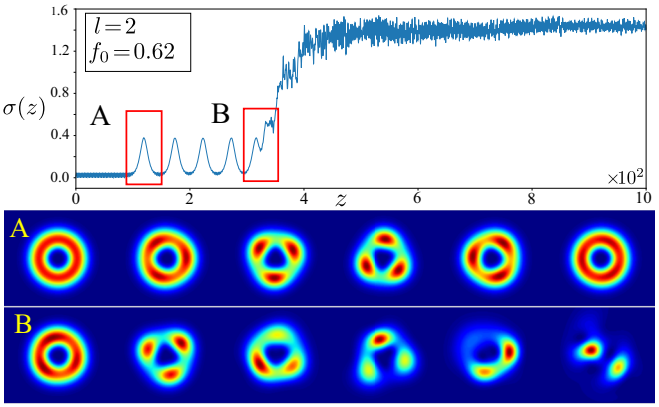

FIG. 4. A recurrent vortex and its eventual disintegration. Top: An example ($l = 2$, $f_0 = 0.62$) of long-distance evolution of $\sigma(z)$. Bottom: The $|\psi_{\rm vort}|^2$ profile for several values of z.

IV. QUALITATIVE SIMILARITIES TO FPUT RECURRENCES

The FPUT recurrence is an oscillation in which nonlinear dynamics plays an essential role. One has an ordered initial state that, due to interactions, gets initially disordered. Eventually, interactions cooperate to restore, almost perfectly, the initial configuration. The A frames of Figs. 3 and 4 clearly resemble this kind of behavior. In order to present their findings, FPUT depicted the evolution in time of the energy partition between modes [1]. Similar plots in the 1D NLSE framework were displayed in Ref. [10]. In our 2D case, it is not obvious which definition of the modes would be the most appropriate and, thus, we will not follow that approach in the present contribution. Notice, however, that one could (partially and heuristically) devise the setup as a one-dimensional problem along the azimuthal extension of the vortex ring. Then, the resemblance to Ref. [10] is obvious: Modulation instability tends to concentrate the energy but, on evolution, it gets again spread out and the uniform distribution is recovered. In addition, the results of Sec. III share other similarities with the FPUT setup. In this section, we will comment on two of them: the emergence of timescales and the existence of a strong stochasticity threshold.

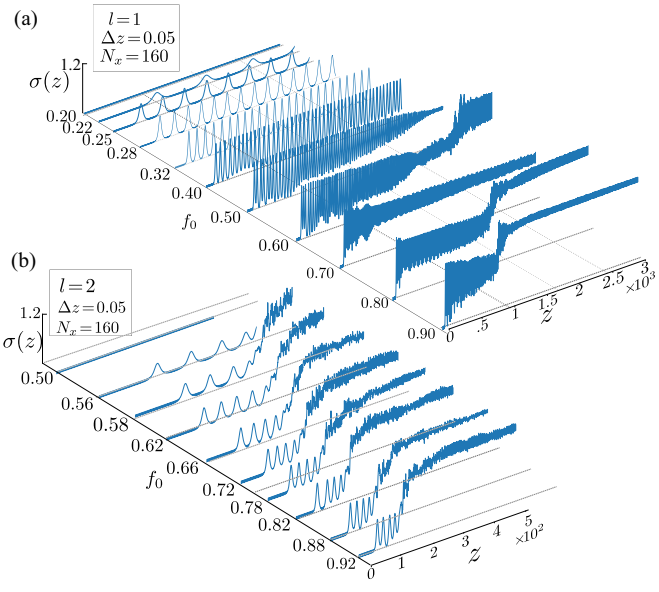

FIG. 5. Comparison of different qualitative behaviors. The evolution of $\sigma(z)$ with different values of f_0, for $l = 1$ (a) and $l = 2$ (b).

A. Timescales

The original FPUT recurrences take place for long-time simulations where "long" is defined in comparison with the inverse frequency of the oscillators, namely the typical timescale of the underlying linear theory. Therefore, due to nonlinear interactions, a new timescale emerges dynamically. To determine whether the revivals in Sec. III are also connected to long propagations, we now discuss the "time" scales of the problem (note that in the optical notation we have used, the propagation distance z plays the role of time).

In particular, two scales can be defined from the eigenstate solution. On the one hand, the typical distance in which the wave function would spread out in the absence of nonlinearities (Rayleigh range), $Z_{\rm Rayl} = R^2/2$. On the other hand, $Z_{\rm spin} = 2\pi R^2 N J^{-1} = 2\pi R^2 l^{-1}$, in relation to the inverse of the angular velocity of the $|\psi|^2$ fluid. We have checked that $Z_{\rm spin}$ provides a fair approximation to the revolution period of the pieces when the vortex-ring splits.

The "linear" scales $Z_{\rm Rayl}$, $Z_{\rm spin}$ should be compared to those emerging from nonlinear evolution. Three such timescales can be defined: $Z_{\rm pert}$ (the time for the perturbative instability to build up, proportional to $\mathrm{Re}[\delta]^{-1}$), $Z_{\rm rec}$ [recurrence time, namely the lapse between two consecutive minima of $\sigma(z)$] and Z_c [the z for the full destruction of the vortex—region C of Fig. 2—that we identify as the onset of chaos, see Sec. IV B]. Indeed, for all recurrent solutions, these nonlinear scales are considerably or much larger than the linear ones, confirming that we are dealing with long-time processes. This is illustrated in Fig. 6, where we depict $Z_{\rm rec}^{-1} \equiv \nu_s$ and Z_c as functions of f_0 for $l = 1$ and 2. It is shown that ν_s grows with f_0 in a roughly linear way. $Z_{\rm rec}$ and Z_c are well above the scales of the linear problem, $Z_{\rm Rayl}$ and $Z_{\rm spin}$, which are of order 1 for a large part of the parameter space. Thus, as in FPUT, there are long timescales that are defined in terms of the results of numerical integration. Namely, they emerge dynamically from the underlying nonlinear properties of the system.

B. A strong stochasticity threshold

In the FPUT systems, the evolution of the system greatly depends on the strength of the nonlinearity. When that parameter is tuned, two kinds of thresholds can be defined, see Ref. [18] for a very illustrative presentation. The stochasticity threshold separates situations in which the overwhelming majority of the phase space trajectories are regular from situations in which energy equipartition and therefore thermalization and chaos are eventually reached. It is well known that FPUT analyzed a situation below the stochasticity threshold. In fact, if they had introduced a larger perturbation in their computations, then they would not have found their paradoxical results. Typically, the stochasticity threshold plays a role

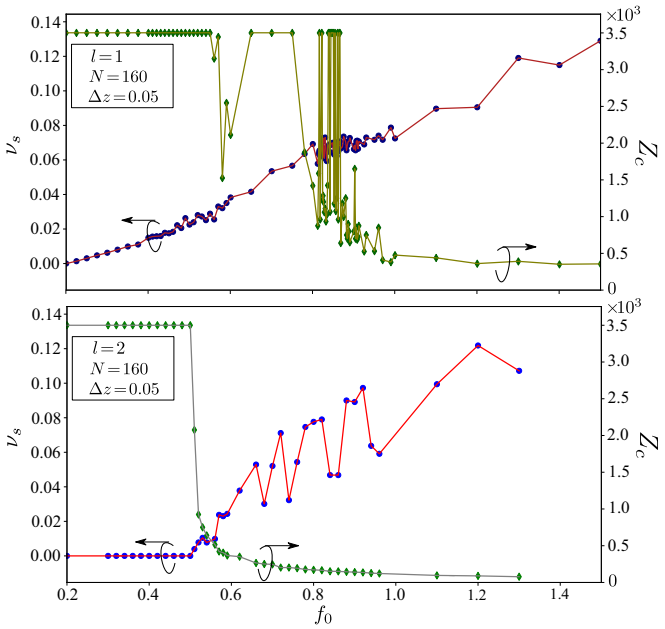

FIG. 6. Timescales. The frequency of revivals ν_s (numerically computed points are represented by circles) and the distance before the onset of chaos Z_c (numerically computed points are represented by diamonds, with those placed at $Z_c = 3500$, meaning that Z_c is larger than that value) as a function of f_0. Increasing f_0 corresponds to increasing the relative importance of the local cubic nonlinearity. The upper panel corresponds to the $l = 1$ family of solutions and the lower panel to $l = 2$.

for integrable systems with a finite number of degrees of freedom and, therefore, it is not relevant for the discussion of this paper. On the other hand, the strong stochasticity threshold is a crossover between weak chaos and strong chaos. The former corresponds to situations in which it takes a long time to reach the chaotic regime: Many recurrences can happen before the memory of the initial condition is lost. Strong chaos means that the chaotic regime is attained rapidly.

In our analysis, the equivalent of the onset of chaos is the disintegration of the initial vortex state. The plots of $\sigma(z)$ in Figs. 2–5 are quite illustrative of this respect. The parameter f_0 controls the strength of the local nonlinearity and tuning it is analog to tuning the strength of the anharmonicity in the FPUT setup. Figure 5 clearly shows that for growing f_0, recurrences becomes weaker and eventually do not appear at all, marking the transition between weak and strong chaos. The plots of $Z_c(f_0)$ in Fig. 6 illustrate this crossover. These results could be compared with Figs. 4 and 5 of Ref. [18] (noting that the Lyapunov exponents are, roughly speaking, inversely proportional to the time lapse before the onset of chaos). For $l = 2$, the crossover is smooth. For $l = 1$, the function $Z_c(f_0)$ is rather fractal in the transition region from the distinctly recurrent solutions to the distinctly nonrecurrent ones. In itself, this is a manifestation of the chaotic nature of nonlinear evolution, being reminiscent of the qualitative behavior of transitions in other setups (see Ref. [39] for a recent example).

In view of this discussion, we conclude that the upper bounds of the recurrent f_0 intervals can be identified with a strong stochasticity threshold [40], providing a remarkable link with FPUT dynamics. Notice that strong stochasticity thresholds are generic in Hamiltonian systems with many degrees of freedom [18].

V. TOWARD A PHYSICAL IMPLEMENTATION

The spatial dynamics of laser beams is an appealing option for the experimental implementation of the phenomena described above. Poisson nonlinearity arises naturally in thermo-optical media, Φ being related to temperature gradients that affect the refractive index (a similar nonlinearity has also been described within nematic crystals [41]). This has attracted attention recently because it facilitates an optical analog of gravitational processes [42]. Vortex-ring states have been created and studied with different purposes [29,43,44]. In all these cases, the cubic (Kerr) term is negligible. However, it was recently suggested [34] that it may be enhanced by suitably doping the medium with nanoparticles and/or by using pulsed lasers in order to produce an interplay between a fast and a slow nonlinearity [45]. While such a procedure has not yet been demonstrated, observing FPUT recurrences is a strong motivation for its experimental realization.

Let us briefly discuss a rough estimation of a setup that would correspond to the examples of Sec. III. In order to connect the dimensionless quantities to physical properties, we can use the relations derived in Sec. II of Ref. [34]. Consider a laser beam with $\lambda = 488$ nm propagating through lead glass, with thermal conductivity $\kappa = 0.7$ W/(mK), thermo-optic coefficient $\beta = 14 \times 10^{-6}$ K^{-1}, linear refractive index $n_0 = 1.8$, linear absorption coefficient $\alpha = 0.01$ cm^{-1} [29], and second-order nonlinear refractive index $n_2 = 2.2 \times 10^{-19}$ m^2/W [45]. Let us assume that the enhancement of the local nonlinearity corresponds to a factor of 2000, presumably achievable with typical Q-switching parameters such as 10 ns pulse duration and 50-kHz repetition rate. Employing these values in the expressions of Ref. [34], we find that the eigenstate of Fig. 2 ($l = 1$, $P \approx 3.2$, $R \approx 1.4$) would have an average power of 24 W and a vortex-ring radius of 16 μm, whereas the one of Fig. 3 ($l = 1$, $P \approx 1.7$, $R \approx 2.0$) would correspond to 13 W and 24 μm and the one of Fig. 4 ($l = 2$, $P \approx 4.8$, $R \approx 1.8$) to 37 W and 21 μm. The propagation distance for a full decay and revival process would be approximately 38 cm in the case of Fig. 3 and 16 cm for the one of Fig. 4. Notice that enhancing n_2 reduces the needed average power but also augments the dimensionful counterpart of z. The mentioned benchmark values indicate that the observation of one or a few revivals might be feasible in a setup of this sort. On the other hand, implementing longer propagations with as many revivals as those shown in Fig. 3 seems a rather far-fetched possibility.

VI. CONCLUSION AND OUTLOOK

Much effort has been devoted to understanding the dynamics of vortex solitons [28]. In the present work, we have computed the lowest-lying vortex-ring eigenstates of the NLSE with local cubic and Poisson focusing nonlinearities. We have found nontrivial and robust nonlinear oscillations between linearly unstable vortex rings and azimuthons (see also Ref. [21]). In general, the presence of competing

nonlinearities leads to interesting dynamical processes that do not manifest in simpler models (see, e.g., Refs. [46,47]). In the present case, this nonlinear competition allows for the tuning of a parameter that, for a given topological order, continuously connects different solutions within the family. We have found an intriguing structure in the parameter space, with transitions among stability, recurrent instability, and nonrecurrent instability. Thus, our discussion addresses a case nonlinear revivals with similarities to previous works [21–26] but with its own peculiarities, such as the robustness of the oscillation and the possibility of tuning the dynamics by modifying the relative strength of the nonlinear terms.

Even if these results are interesting on their own right, we have also emphasized the qualitative similarities with FPUT dynamics of certain features of our setup. The aforementioned tunable parameter plays the role of the strength of the initial perturbation of FPUT. Remarkably, we have found that the transition between recurrent and nonrecurrent solutions presents neat qualitative resemblances to the strong stochasticity threshold. Moreover, we emphasize that, taking into account the analogy to the FPUT system, interesting insights for the dynamics of the system can be developed.

Appealing lines of further inquiry arise. First, it would be useful to find a better theoretical characterization of the involved nonlinear dynamics, maybe in terms of a homoclinic connection as in the case of [48]. A better understanding of the family of azimuthons, along the lines of Ref. [32], should also be interesting. Finding and analyzing similar behaviors in other cases (e.g., different nonlinearities, different dimension, etc.) would be helpful to shed light on the possible qualitative connections with FPUT results. For instance, one may consider a case in which integrability is weakly broken by nonlocal terms [49] or a scenario in which multisoliton dynamics can be approximated by interacting point particles [50], a situation in which an FPUT-like set of ordinary differential equations might be approximately engineered. The three-dimensional generalization of the present model also deserves further study [51]. And, certainly, providing an experimental realization of the discussed vortex revivals would be fascinating. Thus, we hope that the present work will pave the way for research avenues that may shed new light on the implications of the "little discovery" of FPUT in connection to the compelling dynamics of nonlinear vortices and/or solitonic states supported by nonlocal interactions.

ACKNOWLEDGMENTS

We thank two anonymous referees for putting forward a number of references that have greatly improved the presentation of our results. This work is supported by Grant No. FIS2017-83762-P from Ministerio de Economía y Competitividad (Spain) and Grant No. ED431B 2018/57 from Consellería de Educación, Universidad y Formación Profesional (Xunta de Galicia).

[1] E. Fermi, P. Pasta, S. Ulam, and M. Tsingou, Studies of the Nonlinear Problems, Technical Report No. LA-1940, Los Alamos Scientific Laboratory, New Mexico, 1955.
[2] J. Ford, Phys. Rep. **213**, 271 (1992).
[3] G. Berman and F. Izrailev, Chaos **15**, 015104 (2005).
[4] T. Dauxois, M. Peyrard, and S. Ruffo, Eur. J. Phys. **26**, S3 (2005).
[5] T. Dauxois, Phys. Today **61**(1), 55 (2008).
[6] A. Ribal, A. V. Babanin, I. Young, A. Toffoli, and M. Stiassnie, J. Fluid Mech. **719**, 314 (2013).
[7] V. Balasubramanian, A. Buchel, S. R. Green, L. Lehner, and S. L. Liebling, Phys. Rev. Lett. **113**, 071601 (2014).
[8] E. Kuznetsov, Dokl. Akad. Nauk SSSR **236**, 575 (1977).
[9] N. Akhmediev and V. Korneev, Theor. Math. Phys. **69**, 1089 (1986).
[10] K. Hammani, B. Wetzel, B. Kibler, J. Fatome, C. Finot, G. Millot, N. Akhmediev, and J. M. Dudley, Opt. Lett. **36**, 2140 (2011).
[11] E. A. Kuznetsov, JETP Lett. **105**, 125 (2017).
[12] B. Kibler, A. Chabchoub, A. Gelash, N. Akhmediev, and V. E. Zakharov, Phys. Rev. X **5**, 041026 (2015).
[13] O. Kimmoun, H. Hsu, H. Branger, M. Li, Y. Chen, C. Kharif, M. Onorato, E. Kelleher, B. Kibler, N. Akhmediev, and A. Chabchoub, Sci. Rep. **6**, 28516 (2016).
[14] J. Beeckman, X. Hutsebaut, M. Haelterman, and K. Neyts, Opt. Express **15**, 11185 (2007).
[15] G. Van Simaeys, P. Emplit, and M. Haelterman, Phys. Rev. Lett. **87**, 033902 (2001).
[16] X. Hu, W. Chen, Y. Lu, Z. Yu, M. Chen, and Z. Meng, IEEE Photon. Technol. Lett. **30**, 47 (2018).
[17] A. Mussot, A. Kudlinski, M. Droques, P. Szriftgiser, and N. Akhmediev, Phys. Rev. X **4**, 011054 (2014).
[18] M. Pettini, L. Casetti, M. Cerruti-Sola, R. Franzosi, and E. G. D. Cohen, Chaos **15**, 015106 (2005).
[19] M. Guasoni, J. Garnier, B. Rumpf, D. Sugny, J. Fatome, F. Amrani, G. Millot, and A. Picozzi, Phys. Rev. X **7**, 011025 (2017).
[20] N. N. Akhmediev, D. R. Heatley, G. I. Stegeman, and E. M. Wright, Phys. Rev. Lett. **65**, 1423 (1990).
[21] S. Skupin, O. Bang, D. Edmundson, and W. Krolikowski, Phys. Rev. E **73**, 066603 (2006).
[22] D. Buccoliero, A. S. Desyatnikov, W. Krolikowski, and Y. S. Kivshar, Phys. Rev. Lett. **98**, 053901 (2007).
[23] D. Buccoliero and A. S. Desyatnikov, Opt. Express **17**, 9608 (2009).
[24] L. A. Toikka and K. A. Suominen, J. Phys. B: At. Mol. Opt. Phys. **47**, 085301 (2014).
[25] W. Wang, P. G. Kevrekidis, R. Carretero-Gonzalez, D. J. Frantzeskakis, T. J. Kaper, and M. Ma, Phys. Rev. A **92**, 033611 (2015).
[26] I. Shomroni, E. Lahoud, S. Levy, and J. Steinhauer, Nat. Phys. **5**, 193 (2009).
[27] W. J. Firth and D. V. Skryabin, Phys. Rev. Lett. **79**, 2450 (1997).
[28] A. S. Desyatnikov, Y. S. Kivshar, and L. Torner, in *Progress in Optics*, edited by E. Wolf (Elsevier, Amsterdam, 2005), Vol. 47, pp. 291–391.
[29] C. Rotschild, O. Cohen, O. Manela, M. Segev, and T. Carmon, Phys. Rev. Lett. **95**, 213904 (2005).
[30] Y. V. Izdebskaya, V. G. Shvedov, P. S. Jung, and W. Krolikowski, Opt. Lett. **43**, 66 (2018).

[31] A. S. Desyatnikov, A. A. Sukhorukov, and Y. S. Kivshar, Phys. Rev. Lett. **95**, 203904 (2005).
[32] F. Maucher, D. Buccoliero, S. Skupin, M. Grech, A. S. Desyatnikov, and W. Krolikowski, Opt. Quant. Electron. **41**, 337 (2009).
[33] Y. V. Kartashov, V. A. Vysloukh, and L. Torner, Opt. Express **15**, 9378 (2007).
[34] A. Navarrete, A. Paredes, J. R. Salgueiro, and H. Michinel, Phys. Rev. A **95**, 013844 (2017).
[35] A. Alexandrescu and J. R. Salgueiro, Comput. Phys. Commun. **182**, 2479 (2011).
[36] J. M. Soto-Crespo, D. R. Heatley, E. M. Wright, and N. N. Akhmediev, Phys. Rev. A **44**, 636 (1991).
[37] E. Figueiras, D. Olivieri, A. Paredes, and H. Michinel, Eur. J. Phys. **39**, 055802 (2018).
[38] See Supplemental Material at http://link.aps.org/supplemental/10.1103/PhysRevE.99.062211 for videos depicting the result of some simulations with $l = 1$, $l = 2$ for different values of f_0.
[39] A. F. Biasi, J. Mas, and A. Paredes, Phys. Rev. E **95**, 032216 (2017).
[40] M. Pettini and M. Landolfi, Phys. Rev. A **41**, 768 (1990).
[41] C. Conti, M. Peccianti, and G. Assanto, Phys. Rev. Lett. **91**, 073901 (2003).
[42] R. Bekenstein, R. Schley, M. Mutzafi, C. Rotschild, and M. Segev, Nat. Phys. **11**, 872 (2015).
[43] T. Roger, C. Maitland, K. Wilson, N. Westerberg, D. Vocke, E. M. Wright, and D. Faccio, Nat. Commun. **7**, 13492 (2016).
[44] D. Vocke, C. Maitland, A. Prain, K. E. Wilson, F. Biancalana, E. M. Wright, F. Marino, and D. Faccio, Optica **5**, 1099 (2018).
[45] H. C. Gurgov and O. Cohen, Opt. Express **17**, 7052 (2009).
[46] A. Paredes, D. Feijoo, and H. Michinel, Phys. Rev. Lett. **112**, 173901 (2014).
[47] F. Maucher, T. Pohl, S. Skupin, and W. Krolikowski, Phys. Rev. Lett. **116**, 163902 (2016).
[48] F. Maucher, E. Siminos, W. Krolikowski, and S. Skupin, New J. Phys. **15**, 083055 (2013).
[49] W. Krolikowski and O. Bang, Phys. Rev. E **63**, 016610 (2000).
[50] A. W. Snyder and D. J. Mitchell, Science **276**, 1538 (1997).
[51] F. Maucher, S. Skupin, M. Shen, and W. Krolikowski, Phys. Rev. A **81**, 063617 (2010).